Gain-Coupled DFB Lasers Versus Index-Coupled and Phase-Shifted DFB Lasers: A Comparison Based on Spatial Hole Burning Corrected Yield

Klaus David, Geert Morthier, Patrick Vankwikelberge, Roel G. Baets, *Member, IEEE*, Thomas Wolf, and Bernd Borchert

***Abstract*—A statistical yield analysis is presented for gain- and index-coupled DFB laser structures, allowing a comparison of their single longitudinal mode (SLM) yield capabilities. For the yield calculations, we take into account the threshold gain difference ΔgL and the longitudional spatial hole burning (SHB).**

By comparing the experimental and theoretical yield of index-coupled DFB lasers, the significance of spatial hole burning for correct yield predictions is illustrated. For the purpose of comparison, yield calculations for various $\lambda/4$-shifted DFB lasers (with low facet reflectivities) are presented in a novel way. The most emphasis, however, is on partly gain-coupled DFB lasers. First, estimations of practical κ_{gain} (gain coupling coefficient) values for gain and for loss gratings are discussed. Then, for low facet reflectivities, the spatial hole burning corrected yield for various κ_{gain} and κ_{index} (index-coupling coefficient) combinations is given. Results for cleaved facets are also presented. In both cases, a large increase of the spatial hole burning corrected yield has been found. For all structures, design criteria for the optimization of the spatial hole burning corrected yield are discussed.

I. Introduction

ADVANCED optical communication systems, especially coherent systems, require stable single-mode lasers with low linewidth [1]. Favorite candidates are DFB lasers. One problem of perfectly AR-coated index-coupled DFB lasers is the degeneracy into two modes, symmetric to the Bragg frequency [2]. One solution to this problem is the use of non-AR-coated facets. This, however, causes a yield problem associated with the uncertainty of the facet phases [3]. Another solution is the introduction of a $\lambda/4$ phase shift. For perfect AR coatings, these lasers show a high yield, which deteriorates rapidly, however, for reflectivities of only a few percent [4]. Another drawback is the high spatial hole burning (SHB) caused by the phase shift [5]. This can be reduced by modulation of the stripe width [6] or multiple phase shifts. The latter type of laser has been extensively studied for various facet reflectivities and positions of the phase shifts in [4].

An alternative approach is the introduction of gain coupling (induced by a gain grating), which has recently been realized experimentally [7], [8]. Purely gain-coupled lasers were treated theoretically in [2] where it was shown that they have one lasing mode exactly at the Bragg frequency (for AR-coated facets), thereby solving the degeneracy problem. In [9], [10], various degrees of gain coupling have been examined. It is shown there that even a small degree of gain coupling enhances the performance considerably in terms of threshold gain difference and removes the degeneracy of an AR-coated DFB laser. Moreover, a complete elimination of spatial hole burning is possible [10]. For non-AR-coated devices, investigations of yield (with no account taken of spatial hole burning) have been published [11], [12] and show a relevant improvement in yield, even for small amounts of gain coupling. First results of spatial hole burning (SHB) corrected yield of partly gain-coupled DFB lasers have been given in [13] and will be extended here. In addition, first experimental [14] and theoretical [13] results show a potential for lower feedback sensitivity compared to other DFB lasers.

The consideration of spatial hole burning is important because this nonlinearity has a strong effect on various performance aspects of DFB lasers. It has been found both experimentally [5] and theoretically [15] that lasers can become multimoded at low or moderate power levels due to strong spatial hole burning. Moreover, it can give rise to a less flat FM response [16], an increased linewidth [17], and nonlinearities of the *P–I* curve. The latter property is crucial in analog systems where low harmonic distortion is desired [18]. This means that spatial hole burning corrected yield gives information of the percentage of lasers with, e.g., low harmonic distortions and not only of the SLM yield.

This paper is organized as follows. Section II presents the basics of the used laser model. Section III illustrates the importance of spatial hole burning for correct yield predictions by comparing experimental to modeled yield

Manuscript received October 17, 1990; revised January 10, 1991. This work was supported by the European RACE Projects R1010 (CMC) and R1069 (EPLOT). The work of G. Morthier was supported in part by the Belgian IWONL. The work of P. Vankwikelberge was supported by the Belgian NFWO.

K. David, G. Morthier, P. Vankwikelberge and R. G. Baets are with the Laboratory for Electromagnetism and Acoustics, University of Gent–IMEC, B-9000 Gent, Belgium.

T. Wolf and B. Borchert are with the Siemens AG Research Laboratories, D-8000 München 83, Germany.

IEEE Log Number 9100215.

0018-9197/91/0600-1714$01.00 © 1991 IEEE

for index-coupled DFB lasers. SHB corrected yield is given in Section IV for phase-shifted DFB lasers, and in Section V for partly gain-coupled DFB lasers. The section about gain coupling includes a discussion of complex coupling coefficients. Finally, the conclusions are summarized in Section VI.

II. The Model

We present here the threshold analysis method which has been used in our yield calculations and which is based on our laser model CLADISS [15], [16].

In most DFB lasers, only the lowest order TE mode will reach threshold. The forward (+) and backward (−) propagating parts of the lateral electrical laser field of this considered TE mode consist of several longitudinal modes (with mode number m) and can be written as

$$E_y^+(x, y, z, t) = \mathrm{Re}\left\{\Phi(x, y) \sum_m E_m^+(z)\, e^{j(\omega_m t - \beta_b z)}\right\}$$

$$E_y^-(x, y, z, t) = \mathrm{Re}\left\{\Phi(x, y) \sum_m E_m^-(z)\, e^{j(\omega_m t + \beta_b z)}\right\} \tag{1}$$

with $\beta_b = \pi/\Lambda$ for a first-order grating. For all longitudinal modes, the same transverse/lateral field distribution $\Phi(x, y)$ is used, which is assumed to be independent of time and of axial position z. The lasing frequency of the mth mode is represented by ω_m. The complex amplitudes E_m^+ and E_m^- satisfy the following coupled-mode equations:

$$\frac{dE_m^+}{dz} + j\Delta\beta_m E_m^+ = j\kappa_{fb} E_m^-$$

$$-\frac{dE_m^-}{dz} + j\Delta\beta_m E_m^- = j\kappa_{bf} E_m^+. \tag{2}$$

κ_{bf} is the coupling coefficient that couples the backward into the forward wave, and it is given by

$$\kappa_{fb} = -j\kappa_{\mathrm{gain}}\, e^{j\Theta} + \kappa_{\mathrm{index}}. \tag{3a}$$

κ_{bf} is the coupling coefficient that couples the forward into the backward wave, and it is then given by

$$\kappa_{bf} = -j\kappa_{\mathrm{gain}}\, e^{-j\Theta} + \kappa_{\mathrm{index}}. \tag{3b}$$

Θ defines the phase between the gain and index grating (see Section V-A). κ_{index} can be chosen to be real, without loss of generality, by choosing the location of the origin of the z axis. Then κ_{gain} and κ_{index} are real numbers representative of the coupling coefficient of the gain and index grating, respectively. It can easily be verified [9] that for the index grating,

$$\kappa_{fb} = \kappa_{bf}^* \tag{3c}$$

and for the gain grating,

$$\kappa_{fb} = -\kappa_{bf}^*. \tag{3d}$$

In addition, the following boundary conditions are satisfied:

$$E_m^+(0) = \rho_1 E_m^-(0)$$

$$E_m^-(L) = \rho_r E_m^+(L)\, e^{(-2j\beta_b L)}. \tag{4}$$

Furthermore, we have

$$\Delta\beta_m = 2\pi n_e/\lambda - \beta_b + \Gamma\Delta\gamma - 0.5j\alpha_{\mathrm{int}} \tag{5}$$

$$\text{with } \Delta\gamma = 2\pi/\lambda(\Delta n_r + j\Delta n_i) = \Delta\gamma_r + j\Delta\gamma_i \tag{6}$$

$$\Delta\gamma_r = -\alpha_{Iw} a(\lambda) N$$

$$\Delta\gamma_i = a(\lambda)N - b(\lambda).$$

All parameters in the above formulas are explained in Table I. The choice of the origin of the z axis is shown in Fig. 1(a); it is taken at the top of the grating. The displacement between the facet and the reference plane at $z = 0$ and $z = L$ is accounted for in the phases of the reflection coefficients ρ_l and ρ_r. The amplitude reflectivity can be written as $\rho_{l/r} = \rho_{l0/r0} \exp(-j2\pi\Delta_{l/r}/\Lambda)$, in which $\rho_{l0/r0}$ are the facet reflectivities (at the left and right facet) and the phasor expresses the phase between the grating and facet; see Fig. 1(a).

The terms Δn_r and Δn_i represent the variations of the real and imaginary parts of the active layer refractive index due to changes of the carrier density. This carrier density N is given by the following subthreshold static rate equation, in which the longitudinal diffusion term has been neglected because the diffusion length is usually short compared to the axial variations (see again Table I):

$$\frac{\eta J}{qd} = \frac{N}{\tau} + BN^2 + CN^3. \tag{7}$$

The amplitude and phase resonances are defined as follows. The laser cavity is divided into two parts, as shown in Fig. 1(b), which can then be replaced by effective reflectivities, ρ_L for the left part and ρ_R for the right part, respectively. Those reflectivities depend on the frequency ω_m and the applied current I. Using the complex roundtrip gain $\rho_L\rho_R$, the phase and amplitude resonance conditions become

$$\rho_L(\omega_m, I)\, \rho_R(\omega_m, I) - 1 = 0. \tag{8}$$

In this way, the threshold analysis reduces to the search of the roots $(\omega_{m,\mathrm{th}}, I_{\mathrm{th},m})$ of the above equation. The couple with the lowest threshold current $I_{\mathrm{th},m}$ defines the laser threshold. The reflection coefficients ρ_L and ρ_R are calculated by means of the propagator matrices of the left and right parts of the cavity.

CLADISS solves (8) by means of a two-step procedure. In the first step, a scanning procedure over a sufficiently wide frequency window is combined with a bisection algorithm for the currents. For each root found with the bisection procedure, CLADISS activates a Newton-

TABLE I

Parameter		Typical Value	
α_{hw}		6	Linewidth enhancement factor
α_{int}	(μm^{-1})	$50 \cdot 10^{-4}$	Internal waveguide losses
B	($\mu m^3/s$)	100	Bimolecular recombination
C	($\mu m^6/s$)	$20 \cdot 10^{-5}$	Auger recombination
d	(μm)	0.12	Active layer thickness
N	(μm^{-3})		Carrier density
$h\nu$	(eV)		Photon energy related to λ
$2\pi\Delta_l/\Lambda$		$[-\pi, \pi]$	Phase between grating and facet at left facet
$2\pi\Delta_r/\Lambda$		$[-\pi, \pi]$	Phase between grating and facet at right facet
Γ		0.5	Power confinement factor in active layer
κ_{index}	(cm^{-1})		Coupling coefficient for index coupling
κ_{gain}	(cm^{-1})		Coupling coefficient for gain coupling
L	(μm)	∓ 300	Laser length
λ	(μm)		Wavelength of the lasing mode
Λ	(μm)	0.2413	Grating period
n_e		3.25	Unperturbed effective refractive index
η		0.8	Current injection efficiency
q	(C)	$1.6 \cdot 10^{-19}$	Electron charge
τ	(s)	$5.0 \cdot 10^{-9}$	Carrier lifetime
ρ_l			Field reflectivity at left facet
ρ_r			Field reflectivity at right facet

$$\text{Gain} = a(\lambda)N - b(\lambda) \quad (\mu m^{-1})$$
$$\text{with} \quad a(\lambda) = 0.88\ 10^{-6}\,(h\nu - 0.752)^{0.913} \quad (\mu m^2)$$
$$b(\lambda) = 1.63.22\,(h\nu - 0.668)^{3.793} \quad (\mu m^{-1})$$

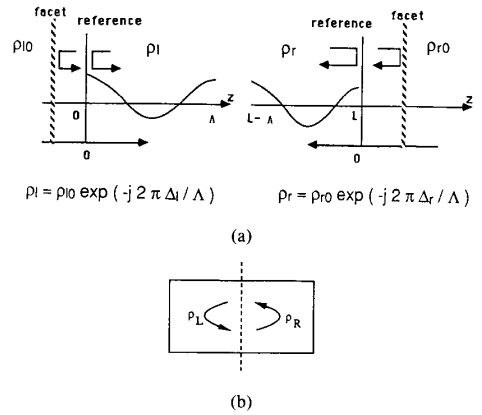

Fig. 1. (a) Phases between grating and facets. (b) Division of the laser cavity into two parts for the calculation of the roundtrip gain.

Raphson algorithm. This second step allows a more accurate determination of the modal thresholds and wavelengths. In addition, by dividing the laser cavity into many small segments and propagating a field of arbitrary strength from segment to segment by using propagator matrices, the longitudinal power profile along the laser cavity is obtained. We express the spatial hole burning as an f number, that is, the ratio of minimum to maximum optical power density along the cavity. $f = 1$ means zero spatial hole burning, and smaller values imply a more inhomogeneous distribution [4]. For a yield calculation of one laser, we take into account $16 \cdot 16$ facet phase combinations.

III. Purely Index-Coupled DFB Lasers

In this section, we present experimental and theoretical yield data. A comparison of both illustrates the importance of spatial hole burning for yield calculations.

The experimental data are obtained from ridge-waveguide DFB lasers with cleaved facets and a first-order grating in the InP substrate emitting at 1.55 μm [19]. The grating is fabricated by conventional holographic exposure and wet chemical etching, resulting in corrugation depths of typically 120 nm. In a single-step LPE process, the grating is overgrown with a quaternary layer, followed by an InP layer, the active, anti-meltback, etch-stopping, ridge, and contact layers. Devices are fabricated using standard techniques [20].

After overgrowth, the corrugation depth is typically 30–50 nm as measured from SEM micrographs. Since controlled variation of the corrugation depth is very difficult in LPE growth, control of the coupling constant is achieved by the composition ($\lambda_g = 1.12$ or 1.2 μm), the thickness ($d = 0.1$–0.3 μm) of the quaternary overgrowth layer, and the thickness of the InP layer below the active layer ($d = 0$–0.15 μm). The coupling constant κ is evaluated according to [21] for a sinusoidal first-order grating:

$$\kappa = \frac{\pi \Delta n \Gamma_{\text{index corrugation}}}{2\lambda}. \tag{9}$$

Δn is the difference in refractive index between the overgrowth layer ($n(Q_{1.12}) = 3.29$ or $n(Q_{1.2}) = 3.34$) and InP ($n \approx 3.17$). $\Gamma_{\text{index corrugation}}$ is calculated by a standard slab-waveguide model as the transverse confinement factor in a layer with a thickness corresponding to the grating depth and with a refractive index of $(n(\text{InP}) + n(Q))/2$.

The experimental yield is defined as the percentage of devices which show a stable single-mode emission (at least 20 dB SMSR, typically more than 30 dB SMSR) at an approximate output power of 5 mW. Since LPE growth inevitably produces local defects, which prevents devices located there from correct operation, all lasers with threshold currents above 100 mA or differential efficiencies below 0.02 W/A per mirror are omitted from the statistics. Typically, about 50 devices are taken into account for each κL value. The comparison of the experimental yield to the conventional theoretical yield shows a large discrepancy for higher κL values, as seen in Fig. 2(a). The calculation of conventional yield is performed for a number of facet phases, and the yield is defined as the percentage of cases where the threshold gain difference ΔgL exceeds a given value, as in [3]. To find an explanation for this discrepancy, we will look more closely at the theoretical calculations.

Fig. 3(a) shows the modeling result for $\kappa L = 1$ and both facets cleaved. In addition to the conventional yield curve (the $f \geq 0$ curve), SHB corrected yield curves are also given ($f \geq 0.2$, 0.4, 0.6, and 0.8, which is in order of

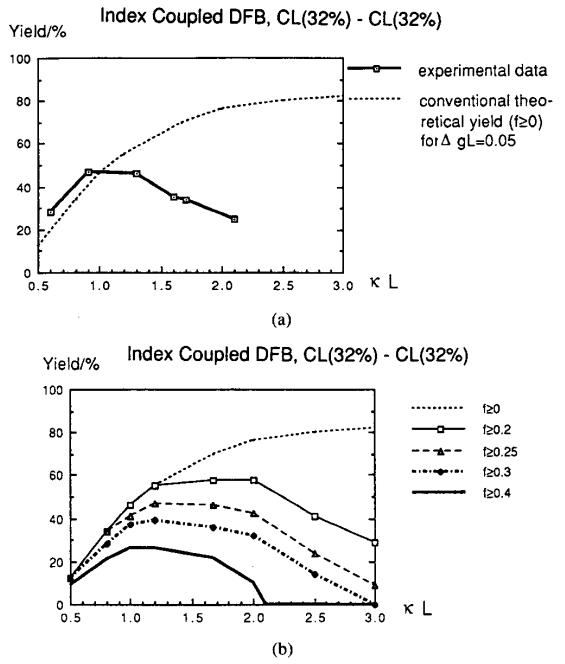

Fig. 2. (a) The comparison between experimental and theoretical yield (not SHB, $f \geq 0$) shows a large discrepancy for larger κL values. (b) SHB corrected yield calculations for five different amounts of spatial hole burning ($f \geq 0$ corresponds to the conventional, uncorrelated yield), all for $\Delta gL \geq 0.05$.

decreasing spatial hole burning). In general, no simple relation between f and ΔgL is found. Fig. 3(b) and (c) give the yield curves for $\kappa L = 1.5$ and 3, respectively. The three conventional yield curves agree very well with other published theoretical results (e.g., [3]). If low spatial hole burning is required, a significant reduction of the yield can be observed.

As a critical value for single-mode operation, $\Delta gL \geq 0.05$ is sometimes used in the literature; see [4], [5]. A summary of the yield for $\Delta gL \geq 0.05$ and 5 f numbers is given in Fig. 2(b). According to the conventional yield curve, it would be advantageous to increase κL, until for very high κL values, the yield drops [3]. By considering spatial hole burning, the situation is quite different, and smaller κL values become favorable, as seen in Fig. 2(b). Indeed, these SHB corrected yield curves give a good prediction of the experimentally observed trend; compare to Fig. 2(a). For κL values larger than about 1.6, the $f \geq 0.3$ curve gives a good fit with the experimental data. For smaller κL values, it predicts a slightly too small yield. This is due to the fact that for smaller κL values, spatial hole burning becomes less and less important for the performance of the laser, until for $\kappa L \approx 0$ (Fabry–Perot), it has no influence anymore. This can also be observed in Fig. 2(b) because the difference between the conventional yield curve and the SHB corrected yield curves decreases with decreasing κL. For the first two experimental points in Fig. 2(a), the $f \geq 0.2$ curve should therefore give the

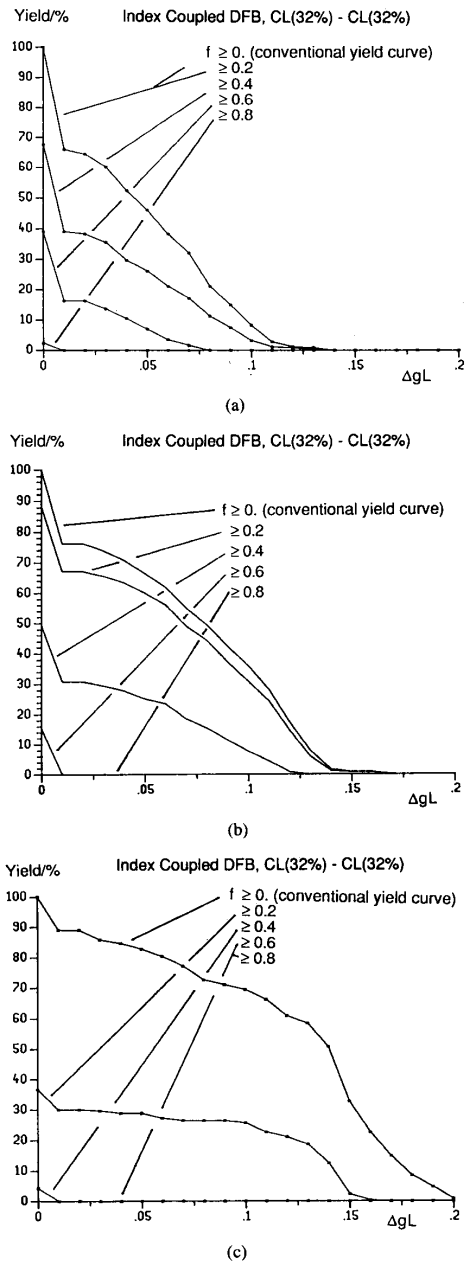

Fig. 3. Yield of index-coupled DFB with both facets cleaved (32% reflectivity). (a)–(c): $\kappa L = 1$, 2, and 3, respectively.

correct yield. The slight deviation can be attributed to the inaccuracies of the experimental κL values.

In summary, by taking spatial hole burning (SHB) into account, the discrepancy between experiment and theory can be explained, and correct trends of the yield can be obtained theoretically.

One simple method to improve the relatively poor yield of the former lasers is the application of an AR coating

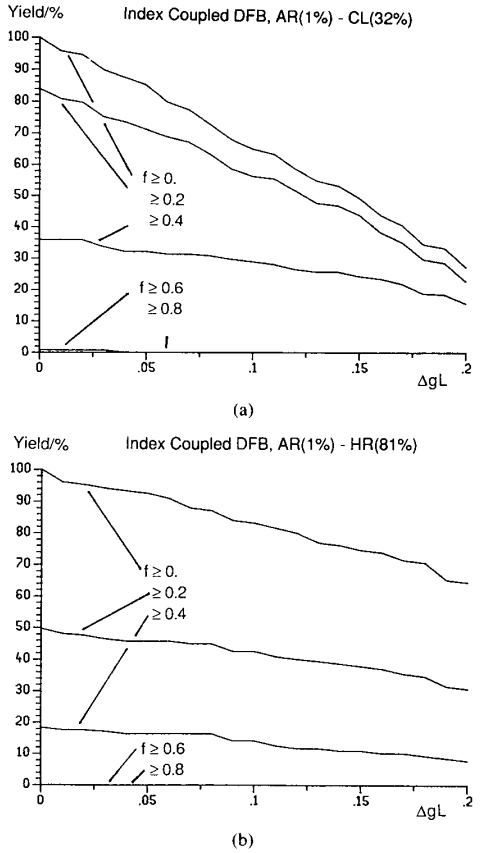

Fig. 4. Yield of index-coupled DFB with $\kappa L = 1.5$ and one facet with 1% reflectivity. (a) Reflectivity of the other facet is 32%, (b) 81%.

and/or a high-reflectivity coating. This has been shown in [22] with conventional yield calculations. In [23], AR-coated/cleaved DFB lasers have been analyzed taking SHB into account. As can be seen in Fig. 4(a), a relevant improvement for ΔgL results by applying one AR coating. Even further improvement of ΔgL can be obtained by increasing the reflectivity of the cleaved facet (see also [4]); compare Fig. 4(a) and (b). A similar laser as in Fig. 4(b) has already been studied both experimentally and theoretically in [24]. There, an experimental yield of 53% is reported, which is lower than their theoretical prediction. In [24], the reason for this difference was unknown. It can be understood by a closer look at Fig. 4(b). For $f \geq 0.2$ and $\Delta gL \geq 0.05$, the calculated yield gives a good prediction of the experimental yield, and it is considerably smaller than the conventional theoretical yield. For still higher reflectivities, the laser becomes similar to a folded $\lambda/4$-shifted DFB, which leads us to the next section.

IV. Phase-Shifted DFB Laser

The $\lambda/4$-shifted DFB laser with the lowest spatial hole burning has been found to have a κL of 1.25 (for perfect AR coatings!) as reported by Soda [5]. Our yield calcu-

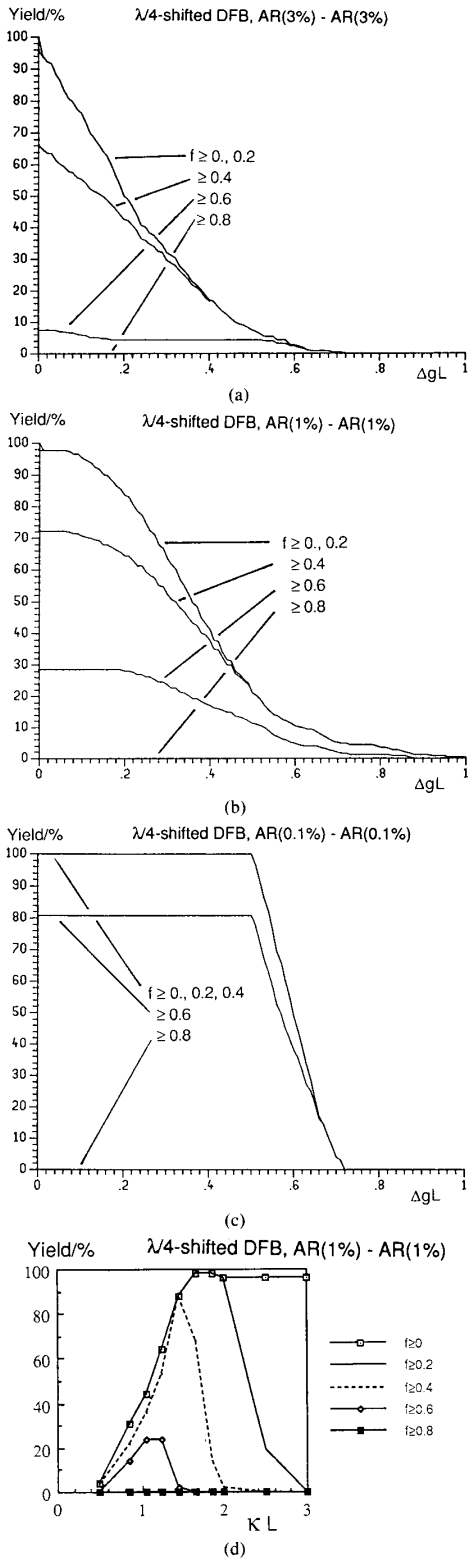

Fig. 5. Yield of $\lambda/4$-shifted DFB with $\kappa L = 1.25$. The reflectivity at both facets is 3, 1, and 0.1% for (a)–(c), respectively. (d) SHB corrected yield of $\lambda/4$-shifted DFB for $\Delta gL \geq 0.3$ and 1% facet reflectivity at both facets.

lation for this optimized $\lambda/4$-shifted DFB laser with 3, 1 and 0.1% reflectivity is shown in Fig. 5(a)–(c) (see also [4]). Notice the relevant improvement of the SHB corrected yield in comparison to the former lasers. In addition, the improvement of yield, especially in terms of spatial hole burning reduction, can be seen for reduced facet reflectivities (see [4]). But even for 0% reflectivity, the f number cannot be improved above about 0.7. For applications where higher f numbers are necessary, multiple-phase-shifted DFB lasers of corrugation pitch-modulated DFB lasers can be a solution [4]. For a further comparison to partly gain-coupled DFB lasers (see Section V-B), we also present the SHB corrected yield for $\Delta gL \geq 0.3$ as a function of κL; see Fig. 5(d). It can be seen that for $f \geq 0.2$–0.3, the optimum becomes $\kappa L \approx 1.9$ rather than 1.25. This shows the usefulness of a representation as in Fig. 5(a)–(c) because for a wide variety of different criteria (concerning f and ΔgL), the yield can be seen.

V. Partly Gain-Coupled DFB Lasers

A. Complex Coupling Coefficient

Before we examine the yield of this type of laser, we will first discuss gain gratings. Basically, two possibilities exist for realizing a gain grating: a periodic gain variation (with the problem that κ_{gain} depends on the injection level) or an absorption grating, meaning a periodic loss variation along the laser cavity (with the advantage of an injection level independent κ_{gain}, but with the disadvantage of higher average losses). The following SHB corrected yield calculations (Section V-B and V-C) are valid for both types. Both gratings have been realized, and more details about them can be found in [8], [12]. In [8], an experimental κ_{gain} of about 40/cm with almost pure gain coupling is reported. This is achieved by a grating between two cladding layers defining a second grating at the following active layer interface. This second grating causes a periodic modulation of the confinement factor, and therefore of the gain. The contribution to κ_{index} of the two gratings cancels because of an appropriate phase between both.

To get a feeling of how to realize κ_{gain} values, we will first briefly review the calculation of κ_{index}, and then, based on this, estimates for κ_{gain} are given and a new possibility for enhancing the κ_{gain} values is presented. The deviation of the coupled-mode equations for a slab waveguide with grating perturbation gives the well-known result for κ_{index} [21]:

$$\kappa_{index} = \frac{k_0^2}{2\beta} \int_{\text{index corrugation}} \varepsilon(x) \Delta\epsilon \, E^2(x) \, dx \qquad (10)$$

where $k_0 = 2\pi/\lambda_0$ is the free-space wavenumber, $\varepsilon(X)$ is the appropriate Fourier component of the perturbation along the longitudinal coordinate (appropriate to the Bragg scattering), $\Delta\epsilon = \Delta\epsilon_{index} = n_1^2 - n_2^2$, n_1 and n_2 being the refractive indexes above and below the grating interface, and we assume normalized optical fields ($E(x)$). If $\varepsilon(X)$ is constant, (10) can be rewritten as

$$\kappa_{index} = \frac{k_0^2}{2\beta} \varepsilon (n_1^2 - n_2^2) \Gamma_{\text{index corrugation}} \qquad (11)$$

with $\Gamma_{\text{index corrugation}}$ being the confinement factor of the rectangular index grating. Considering a first-order rectangular grating with typical values (see, e.g., [21]), one can give the following estimates:

$$\frac{k_0^2}{2\beta} \approx 1/\mu\text{m}, \qquad \varepsilon = 1/\pi,$$

$$n_1^2 - n_2^2 \approx 3.6^2 - 3.4^2 \approx 1.4,$$

$$\Gamma_{\text{index corrugation}} \approx 1\text{–}3 \; 10^{-2}, \qquad \lambda \approx 1 \; \mu\text{m}.$$

This gives, for $L = 300$ μm, $\kappa_{index} L \approx 1$–$3$.

The analysis above can be repeated for pure gain coupling. $\Delta\epsilon$ is now given by $\Delta\epsilon_{gain} = n_e \Delta g_g / k_0$, and $\Gamma_{\text{index corrugation}}$ becomes Γ_g, the confinement factor of the gain grating. n_e is the effective refractive index ($\beta = n_e k_0$). This results in

$$\kappa_{gain} \approx 1/6 \cdot \Delta g_g \Gamma_g. \qquad (12)$$

Δg_g is given by

$$\Delta g_g = (g_{mat} - \alpha_{active}) + \alpha_{active} \qquad (13)$$

with g_{mat} being the material gain and α_{active} the losses in the active layer. Before evaluating (12), we will first look at the value for the material gain g_{mat} required for laser operation:

$$g_{modal} = \Gamma_{active}(g_{mat} - \alpha_{active}) - \Gamma_{cladding} \alpha_{cladding} \qquad (14)$$

where

g_{modal} = modal power gain
Γ_{active} = confinement factor of the active layer
$\Gamma_{cladding}$ = confinement factor of the cladding layer
$\alpha_{cladding}$ = losses in the cladding layers.

Setting $\alpha_{cladding} = 0$ and taking the values $g_{modal} = 100/\text{cm}$, $\Gamma_{active} = 0.5$ [see Fig. 6(a)], and $\alpha_{active} \approx 250/\text{cm}$. For the hypothetical gain grating sketched in Fig. 6(a) (where $\Delta g_g = g_{mat}$), this results in a κ_{gain} value of about 42/cm. A problem with these estimates is that g_{modal} is a function of κ_{gain} (see, e.g., [9]). For a purely gain-coupled DFB with perfect AR coatings, curve a in Fig. 6(c) sketches this relation. Curve b shows the proportionality between κ_{gain} and g_{modal}. The intersection between curves a and b then gives a self-consistent operation point at and above threshold. For a κ_{gain} of about 42/cm, it is shown that the above-chosen g_{modal} is too large. To overcome this problem, we look at the structure in Fig. 6(b) where an additional lossy cladding layer is introduced. With $\Gamma_{cladding} = 0.2$, $\alpha_{cladding} = 650/\text{cm}$, $\Gamma_{active} = 0.4$, $\Gamma_g = 0.8$, and $g_{modal} \approx 0/\text{cm}$, we get for $g_{mat} \approx 375/\text{cm}$ a $\kappa_{gain} \approx 50/\text{cm}$. This means a parallel shift of curve b [Fig. 6(c)] to curve c. The intersection point between curves a and c is now a self-consistent solution. For $\kappa_{gain} L \approx 1.57$, g_{modal} indeed drops to almost

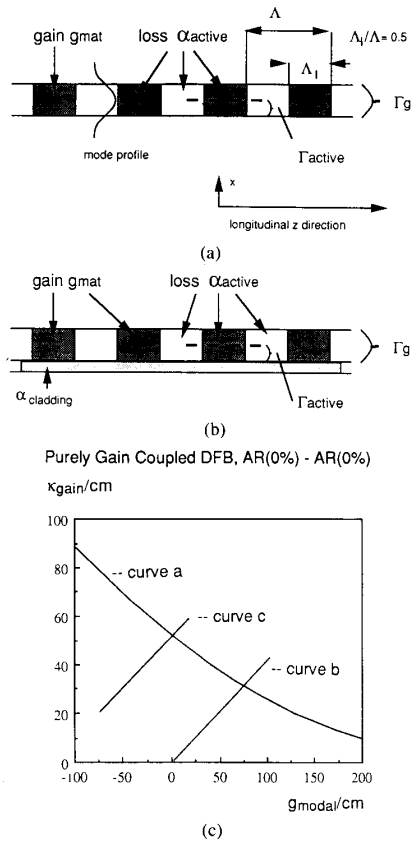

Fig. 6. (a) Structure for the estimation of κ_{gain} for gain coupling and (b) with additional lossy cladding layer. (c) Relation between κ_{gain} and the modal gain g_{modal}.

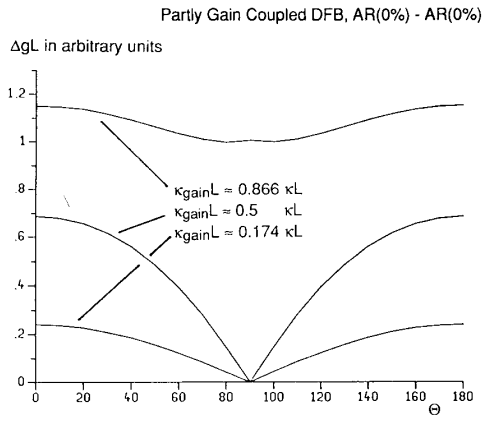

Fig. 7. Threshold gain difference ΔgL (in arbitrary units) for three amounts of κ_{gain}. This illustrates the influence of the phase θ between the gain and index grating on ΔgL. κL equals $(\kappa_{gain}^2 + (\kappa_{index}^2)^{1/2}$ and is kept constant.

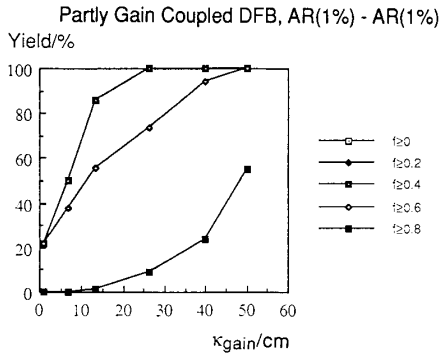

Fig. 8. SHB corrected yield of partly gain-coupled DFB lasers for $\Delta gL \geq 0.3$, 1% facet reflectivity at both facets, and an optimized $\kappa_{index}L$ (around 1.7 ± 0.2).

zero (see [2], [10]). From these arguments, it is clear that high κ_{gain} values can only be achieved at the expense of the threshold current [25].

In summary, in semiconductor materials where material gains of $g_{mat} \approx 2\text{–}4 \cdot 100/\text{cm}$ are possible, significant gain-coupling κ_{gain} values should be possible. To enhance a high g_{mat}, even for low g_{modal}, a lossy cladding layer might be useful.

In cases where κ_{gain} and κ_{index} are caused by separate gratings, any phase Θ [see (3a) and (3b)] between the gain grating and the index grating becomes possible. From Fig. 7, we learn that phase 0 and π are most advantageous, particularly for lower amounts of gain coupling. The only difference between these two cases is a different lasing wavelength (λ): for $\Theta = 0°$, λ is shorter than the Bragg wavelength, and for $\Theta = 180°$, λ is longer. These are actually the two possible cases if both κ_{gain} and κ_{index} are caused by one grating. The presented yield calculations are valid for $\Theta = 0°$ and $\theta = 180°$.

B. Partly Gain-Coupled DFB Lasers with Low Facet Reflectivities

In [11], [12], the conventional yield of partly gain-coupled DFB lasers has been studied. A significant increase of both ΔgL and yield, even for cleaved facets, and small amounts of gain coupling were the major results. This improvement in yield, and also other improvements of gain-coupled DFB lasers, can intuitively be understood by the following reasoning (see also [10]). In gain-coupled DFB lasers, it is essential to consider the interaction between the standing waves along the laser cavity and the periodic variation of the gain (or loss). This explains, for example, the fact that even negative threshold gain values are possible. The standing-wave pattern and the gain pattern "try" to maximize (or minimize) their overlap (lowest threshold gain!). This mechanism, not present in index-coupled DFB lasers, works against the influence of the facet/phase contribution, resulting in a higher yield.

Here we will consider the spatial hole burning as well. In [26], the threshold gain difference requirements of single-mode lasers for several optical systems have been studied, and values up to $\Delta gL \approx 0.24$ have been found necessary. To be on the safe side, we will now also use $\Delta gL \geq 0.3$ as a threshold gain difference criterion.

In Fig. 8, the SHB corrected yield for $\Delta gL \geq 0.3$, 1% facet reflectivity, and various κ_{gain} values is given. The

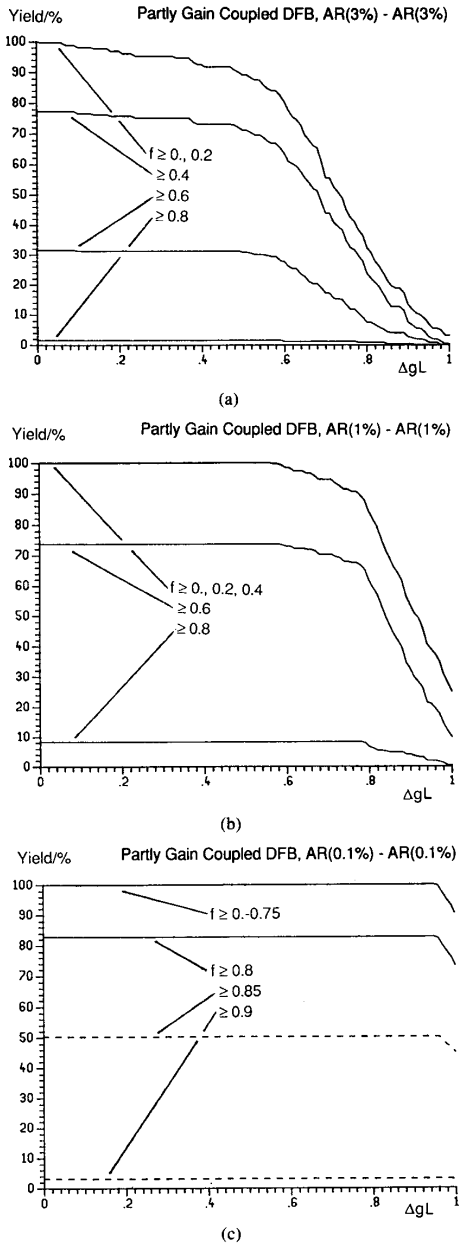

Fig. 9. Yield of partly gain-coupled DFB with $\kappa_{gain} = 26.18/cm$, $\kappa_{index} = 49/cm$. The reflectivity at both facets is 3, 1, and 0.1% for (a)–(c), respectively.

κ_{index} values are the optimized values as given in [10]. Already, for $\kappa_{gain} \geq 26.18/cm$, the yield for $f \geq 0.6$ is about 74%. This is more than twice the yield of the optimized $\lambda/4$-shifted DFB; see Fig. 5(a). Because of the superior yield figures of this last laser, we will look at it, and study the influence of various facet reflectivities and various amounts of κ_{index}. In Fig. 9(a)–(c), the yield for 3, 1, and 0.1% facet reflectivity at both facets is given

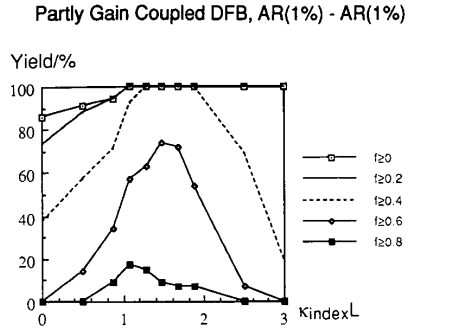

Fig. 10. SHB corrected yield of partly gain-coupled DFB lasers for $\Delta gL \geq 0.3$, $\kappa_{gain} = 26.18/cm$, and 1% facet reflectivity at both facets.

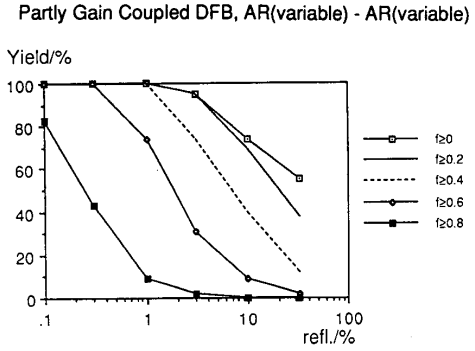

Fig. 11. SHB corrected yield of partly gain-coupled DFB lasers for $\Delta gL \geq 0.3$, $\kappa_{gain} = 26.18/cm$, and $\kappa_{index} = 49/cm$.

[compare to Fig. 5(a)–(c)]. The last figure shows, with 83% yield for $\Delta gL \geq 0.3$ and $f \geq 0.8$, a performance which is unattainable for any $\lambda/4$-shifted DFB. Fig. 10 shows the influence of $\kappa_{index}L$ on the yield; compare to Fig. 5(d). It can be seen that the partly gain-coupled DFB is less sensitive to $\kappa_{index}L$ inaccuracies than, e.g., the $\lambda/4$-shifted DFB, and $\kappa_{index}L$ contributions between about 1 and 2 can be tolerated without a significant decrease of the yield.

C. Partly Gain-Coupled DFB Lasers with High Facet Reflectivities

Given the excellent yields of partly gain-coupled DFB lasers with AR coatings, one may wonder how the yield behaves for non-AR-coated facets. Fig. 11 shows the SHB corrected yield for $\Delta gL \geq 0.3$, $\kappa_{gain} = 26.18/cm$, $\kappa_{index} = 49/cm$, and various facet reflectivities. In general, the yield decreases with increasing facet reflectivity. For cleaved facets, the SHB yield is shown in detail in Fig. 12. This shows the relevant improvement of SHB corrected yield in comparison to pure index-coupled DFB lasers; see Section III. In Fig. 13, the influence of κ_{index} on the yield can be seen. Two things can be observed: first, the yield does not critically depend on κ_{index}, and second for small κ_{index} values, low spatial hole burning can be

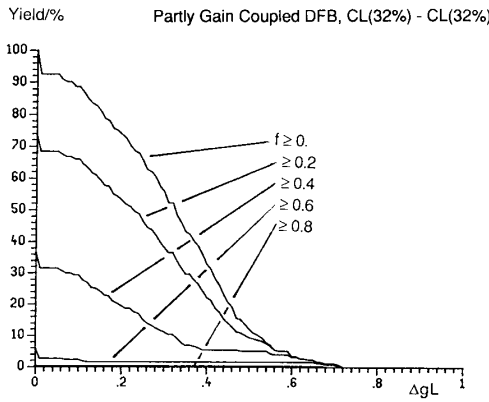

Fig. 12. Yield of partly gain-coupled DFB with $\kappa_{gain} = 26.18/cm$, $\kappa_{index} = 49/cm$, and both facets cleaved.

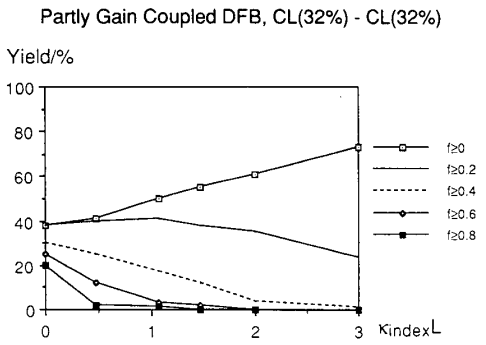

Fig. 13. SHB corrected yield of partly gain-coupled DFB lasers for $\Delta gL \geq 0.3$, $\kappa_{gain} = 26.18/cm$, and both facets cleaved.

obtained. Finally, the SHB corrected yield for $\Delta gL \geq 0.3$, $\kappa_{index} \approx 0/cm$, cleaved facets, and various κ_{gain} values is given in Fig. 14. A yield of about 30% (for $f \geq 0.8$!) becomes feasible for a DFB with cleaved facets. This shows that AR coatings are not indispensable for gain-coupled DFB lasers, making them even more attractive.

VI. Conclusions

The SLM yield of index-coupled DFB lasers with both facets cleaved (32% reflectivity) and various κL values was studied both theoretically and experimentally. It was found that for κL values larger than about 1.6, the conventional theoretical yield (no consideration of spatial hole burning) and the experimental yield show a large discrepancy. This problem could be solved by taking longitudinal spatial hole burning (SHB) into account. The importance of SHB is also seen by looking at the yield of index-coupled DFB lasers with one AR-coated facet and/or a high-reflectivity coating at the other facet.

Next, $\lambda/4$-shifted SFB lasers were analyzed for low facet reflectivities. It was found that, depending on the facet reflectivity and the degree of allowed SHB, a κL of 1.25 (which is the optimum value for perfect AR coatings) is not always the optimum choice. Small deviations of the facet reflectivities ΔR (already about $\Delta R \approx 1\%$) and the κL value (about $\Delta \kappa L \approx 0.2$) from the optimum design values cause a significant deterioration of the yield.

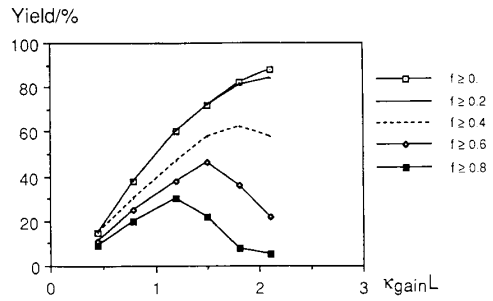

Fig. 14. SHB corrected yield of partly gain-coupled DFB lasers for $\Delta gL \geq 0.3$, $\kappa_{index} = 0/cm$, and both facets cleaved.

Most of the attention in this paper has been devoted to partly gain-coupled DFB lasers. First, estimates for the gain-coupling coefficient κ_{gain} were given. In materials where sufficiently high material gains of a few $100/cm$ are possible, κ_{gain} values of a few $10/cm$ should be attainable, confirming published values of up to $40/cm$ [8]. The influence of the phase between the index and gain grating was shown. Both should be either in phase or out of phase. Next, the SHB corrected yield of partly gain-coupled DFB lasers with low facet reflectivities was analyzed. The results show a high yield with very large ΔgL and small f numbers, unattainable for any $\lambda/4$-shifted or multiple-phase-shifted [4] DFB. In addition, this performance is fairly insensitive to deviations of $\kappa_{gain}L$, large deviations of κ_{index}, as well as moderate deviations of the facet reflectivities from the optimum design values. This should result in a high yield of deviations with high output powers, high SMSR, low harmonic distortion, and low linewidth. Finally, partly gain-coupled DFB lasers with cleaved facets were examined. Especially for low κ_{index} values, combined with sufficiently high κ_{gain} values, a high SHB corrected yield again can be obtained.

References

[1] K. Nosu and K. Iwashita, "A consideration of factors affecting future coherent lightwave communication systems," *J. Lightwave Technol.*, vol. 6, pp. 686-694, 1988.

[2] H. Kogelnik and C. V. Shank, "Coupled-wave theory of distributed feedback lasers," *J. Appl. Phys.*, vol. 43, no. 5, pp. 2327-2335, 1972.

[3] J. Buus, "Mode selectivity in DFB lasers with cleaved facets," *Electron. Lett.*, vol. 21, pp. 179-180, 1985.

[4] J. Kinoshita and K. Matsumoto, "Yield analysis of SML DFB lasers with an axially-flattened internal field," *IEEE J. Quantum Electron.*, vol. 25, pp. 1324-1332, 1989.

[5] H. Soda, Y. Kotaki, H. Sudo, H. Ishikawa, S. Yamakoshi, and H. Imai, "Stability in single longitudinal mode operation in GaInAsP/InP phase-adjusted DFB lasers," *IEEE J. Quantum Electron.*, vol. QE-23, pp. 804-814, 1987.

[6] Y. Nakano and K. Tada, "Analysis, design, and fabrication of GaAlAs/GaAs DFB lasers with modulated stripe width structure for complete single longitudinal mode oscillation," *IEEE J. Quantum Electron.*, vol. 24, pp. 2017–2033, 1988.
[7] Y. Luo, Y. Nakano, K. Ikeda, K. Tada, T. Inoue, H. Hosomatsu, and H. Iwaoka, "Low threshold CW operation in a novel gain-coupled distributed feedback semiconductor laser," in *Tech. Dig., 12th IEEE Semiconductor Laser Conf.*, Davos, Switzerland, Sept. 1990, pp. 70–71.
[8] Y. Luo, Y. Nakano, K. Tada, T. Inoue, H. Hosomatsu, and H. Iwaoka, "Purely gain-coupled distributed feedback lasers," *Appl. Phys. Lett.*, vol. 56, no. 17, pp. 1620–1622, 1990.
[9] E. Kapon, A. Hardy, and A. Katzir, "The effects of complex coupling coefficients on distributed feedback lasers," *IEEE J. Quantum Electron.*, vol. QE-18, pp. 66–71, 1982.
[10] G. Morthier, P. Vankwikelberge, K. David, and R. Baets, "Improved performance of AR-coated DFB lasers by the introduction of gain coupling," *IEEE Photon. Technol. Lett.*, vol. 2, pp. 170–172, Mar. 1990.
[11] K. David, G. Morthier, P. Vankwikelberge, and R. Baets, "Yield analysis of non-AR-coated DFB lasers with combined index and gain coupling," *Electron. Lett.*, vol. 26, pp. 238–239, 1990.
[12] Y. Nakano, Y. Luo, and K. Tada, "Facet reflection independent, single longitudinal mode oscillation in a GaAlAs/GaAs distributed feedback laser equipped with a gain-coupling mechanism," *Appl. Phys. Lett.*, vol. 55, no. 16, pp. 1606–1608, 1989.
[13] K. David, G. Morthier, P. Vankwikelberge, and R. Baets, "Partly gain-coupled versus $\lambda/4$-shifted—DFB laser: A comparison," in *Tech. Dig., 12th IEEE Int. Semiconductor Laser Conf.*, Davos, Switzerland, Sept. 1990, pp. 202–203.
[14] Y. Nakano, Y. Deguchi, K. Ikeda, Y. Luo, and K. Tada, "Resistance to external optical feedback in gain-coupled semiconductor DFB laser," in *Tech. Dig., 12th IEEE Int. Semiconductor Laser Conf.*, Davos, Switzerland, Sept. 1990, pp. 71–72.
[15] P. Vankwikelberge, G. Morthier, and R. Baets, "CLADISS, A longitudinal, multimode model for the analysis of the static, dynamic, and stochastic behavior of diode lasers with distributed feedback," *IEEE J. Quantum Electron.*, vol. 26, pp. 1728–1741, Oct. 1990.
[16] P. Vankwikelberge, F. Buytaert, A. Francois, R. Baets, P. Kuindersma, and C. Frederiksz," Analysis of the carrier induced FM response of DFB lasers: Theoretical and experimental case studies," *IEEE J. Quantum Electron.*, vol. 25, pp. 2239–2254, 1989.
[17] J. E. A. Whiteaway, G. H. B. Thompson, C. J. Armistead, A. J. Collar, S. J. Clements, and M. Gibbon, "The influence of longitudinal mode spatial hole burning on the linewidth and spectrum of $\lambda/4$-phase shifted DFB laser," in *Proc. 11th IEEE Int. Semiconductor Laser Conf.*, Boston, MA, Sept. 1988.
[18] A. Takemoto, H. Watanabe, Y. Nakajima, Y. Sakakibara, S. Kakimoto, H. Namizaki, J. Yamashita, T. Hatta, and Y. Miyake, "Low harmonic distortion distributed feedback laser diode and module for CATV systems," in *Tech. Dig. OFC*, 1990, p. 214.
[19] Th. Wolf, B. Borchert, and M.-C. Amann, "Narrow linewidth metal-clad ridge-waveguide distributed feedback lasers fabricated by a one-step epitaxial growth," *Japan. J. Appl. Phys.*, to be published.
[20] M.-C. Amann and B. Stegmüller, "Narrow-stripe metal-clad ridge-waveguide laser for 1.3 μm wavelength," *Appl. Phys. Lett.*, vol. 62, pp. 1541–1543, 1987.
[21] W. Streifer, D. R. Scifres, and R. D. Burnham, "Coupling coefficients for distributed feedback single- and double-heterostructure diode lasers," *IEEE J. Quantum Electron.*, vol. QE-11, pp. 867–873, 1975.
[22] C. H. Henry, "Performance of distributed feedback lasers designed to favor the energy gap mode," *IEEE J. Quantum Electron.*, vol. QE-21, pp. 1913–1918, 1985.
[23] H. Soda, H. Ishikawa, and H. Imai, "Design of DFB lasers for high-power single-mode operation," *Electron. Lett.*, vol. 22, pp. 1047–1049, 1986.
[24] K. Kobayashi and I. Mito, "High light output-power single-longitudinal-mode semiconductor laser diodes," *J. Lightwave Technol.*, vol. LT-3, pp. 1202–1210, 1985.
[25] K. David, J. Buus, G. Morthier, and R. Baets, "Coupling coefficients in gain coupled DFB lasers: Inherent compromise between coupling strength and loss," *IEEE Photon. Technol. Lett.*, to be published, May 1991.
[26] J. C. Cartledge and A. F. Elrefaie, "Threshold gain difference requirements for nearly single-longitudinal-mode lasers," *J. Lightwave Technol.*, vol. 8, pp. 704–715, 1990.

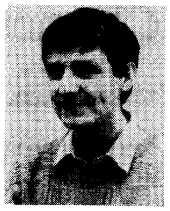

Klaus David was born in Frankfurt/Main, Germany, on September 16, 1961. He received the Diplom Phys. degree from the University of Siegen, Germany, in 1988.

During his studies, he was a research student in the Research Laboratories of Hewlett-Packard, Böblingen, Germany, and STC Technology (STL), Harlow, England. Since 1988 he has been with the Interuniversity Micro-Electronics Centre (IMEC), University of Gent, Gent, Belgium, and is working towards the Ph.D. degree in the Laboratory of Electromagnetism and Acoustics there. His interests include semiconductor lasers and coherent optical systems.

Geert Morthier was born in Gent, Belgium, on March 20, 1964. He received the degree in electrical engineering from the University of Gent in 1987.

He is presently working towards the Ph.D. degree in electrical engineering at the Laboratory of Electromagnetism and Acoustics, University of Gent. His main research interests are the spectral and dynamic properties of semiconductor lasers, and the design of DFB lasers with reduced spatial hole burning.

Patrick Vankwikelberge was born in Gent, Belgium, on May 20, 1962. He received the degree in electrical engineering and the Ph.D. degree from the University of Gent in 1985 and 1990, respectively.

His interests include the dynamic properties of semiconductor lasers and quantum-well lasers.

Roel G. Baets (M'88), for a photograph and biography, see p. 787 of the March 1991 issue of this JOURNAL.

Thomas Wolf was born in Bamberg, Germany, in 1958. He received the Diplom degree in physics in 1985 from the Technical University of Munich, Munich, Germany.

After joining the Research Laboratories of Siemens AG, Munich, in 1985, he worked on laser arrays in the InGaAsP system. Since 1989 he has been involved in the development of narrow-linewidth DFB lasers and tunable laser diodes.

Bernd Borchert was born in Hannover, Germany, on June 13, 1958. He received the Diplom Phys. and the Ph.D. degrees from the University of Hannover, Hannover, Germany, in 1984 and 1987, respectively. His dissertation concerned nonlinear transport properties of hot electrons in short-channel silicon MOSFET's.

Since joining Siemens AG Research Laboratories, Munich, in 1984, he has been engaged in the study of hot-electron effects in silicon MOSFET's. Since 1987 he has been involved in the development of long-wavelength laser diodes, and especially in the design of DFB laser diodes and integrated optical devices.